Synthesis and characterization of binuclear complexes of metals transition of *N*'^{1},*N*'^{4}-bis(1-(pyridin-2-yl)ethylidene)succinohydrazide

ABSTRACT

Six news dinuclear metal transition (Mn(II) (**1**), Fe(II) (**2**), Co(II) (**3**), Ni(II) (**4**), Cu(II) (**5**) and Zn(II) (**6**)) complexes have been synthesized from a new hexadentate Schiff base *N*'^{1},*N*'^{4}-bis(1-(pyridin-2-yl)ethylidene)succinohydrazide (H_2L). The ligand was characterized by elemental analysis, FTIR, UV-visible, ^{1}H NMR and ^{13}C NMR. The synthetized compounds have been investigated by elemental analysis, FTIR and UV-visible spectroscopies, molar conductance and room temperature magnetic moments measurement. The results show that the complexes **1**-**6** are dinuclear neutral electrolytes in DMF. Each of the two mono deprotonated tridentate arms of the ligand are coordinated to one metal ion through one iminolate oxygen atom, one azomethine nitrogen atom and one pyridine nitrogen atom. Octahedral geometries are proposed for all the complexes **1**-**6** formulated as $[(ML)_2]\cdot nH_2O$. The structure of the Ni(II) (**4**) complex is confirmed by X-ray crystallography study.

Keywords: FTIR, UV-visible, acetylpyridine, succinohydrazide, octahedral, X-ray.

1. INTRODUCTION

The interaction of transition metal ions with functionalized ligands is one of the most attractive and potentially useful areas of coordination chemistry [1–4]. Coordination chemistry of transition metals has attracted great interest in various fields of science and technology [1, 5–7]. Ligands containing a hydrazone unit have been particularly studied in recent years, due to their interesting intrinsic properties and their significant chelating capacity [8–10]. Thus, these types of ligands are used to generate coordination compounds with diverse applications [11–14]. These Schiff bases can chelate different metal ions forming mononuclear [15, 16], polynuclear [17, 18] or heteropolynuclear [19–21] complexes. Dihydrazone ligands that are characterized by the presence of two hydrazonic groups linked by a spacer constitute good polydentate chelating agents that can present in several conformations to encapsulate metal ions, generating compounds with particular properties [22–24]. Thus, compounds with biological applications have been reported in the literature [25]. Coordination compounds with catalytic [26], magnetic [26], antimicrobial [27], antifungal [28], antituberculosis [29], and anticancer [30] properties are widely studied. Metal complexes of dihydrazones are also used in biomimetic chemistry for the study of various enzymes [31–33]. Our team has already synthesized and studied the structure of several compounds derived from hydrazonic ligands [34–38]. Therefore, in the continuity of our research work on transition metal complexes, we have synthesized a new dihydrazone ligand whose two arms are connected by a flexible spacer of type $-(CH_2)_4-$, which allows it to have a *syn* or *anti* conformation and a *cis* or *trans* configuration. This ligand allowed the synthesis of six new complexes whose structures are determined by a spectroscopic study (FTIR and UV-visible) and conductimetric and magnetic moments measurements at room temperature of the complexes. The structure of the Ni(II) complex is confirmed by crystallography.

2. MATERIAL AND METHODS

2.1 Starting materials and Instrumentations

2-acetylpyridine, succinohydrazide, manganese chloride hexahydrate, iron chloride tetrahydrate, cobalt chloride hexahydrate, nickel chloride hexahydrate, copper chloride dihydrate and zinc chloride dihydrate were commercial products (from Aldrich) and were used without further purifications. The solvents were

UNDER PEER RE

reagent grade and were purified by usual methods. Elemental analyses were carried out using a VxRio EL Instrument. The FTIR spectra were recorded on a FTIR Spectrum Two of Perkin Elmer (4000–400 cm^{-1}). The UV–Visible spectra were run on a Perkin-Elmer UV/Visible spectrophotometer Lambda 365 (1000–200 nm). The ^{1}H and ^{13}C NMR spectra of the Schiff base were recorded in DMSO-d_6 on a BRUKER 500 MHz spectrometer at room temperature using TMS as an internal reference. The molar conductance of 10^{-3} M solutions of the metal complexes in DMF were measured at 25 °C using a WTW LF-330 conductivity meter with a WTW conductivity cell. Magnetic measurements for complexes were performed at room temperature by using a Johnson Mattey scientific magnetic susceptibility balance (Calibrant: $Hg[Co(SCN)_4]$).

2.2 Synthesis of the ligand H_2L

In a 250 mL round-bottomed flask containing 30 mL of methanol, 2 g (13.7 mmol) of succinohydrazide were added and the mixture was stirred for 30 min before adding 3.31 g (27.4 mmol) of 2-acetylpyridine. The mixture was refluxed for three hours. After cooling, the white solid wass recovered by filtration and washed with ether (2 x 20 mL), then dried in the open air. M.P. 252-254°C. Yield : 89%. ^{1}H NMR (DMSO-d_6, δ(ppm)) : 2.32 (s, 6H, -CH_3), 3.05 (s, 4H, -CH_2), 7.39 (m, 2H, H_{Ar}), 7.79-7.85 (m, 2H, H_{Py}), 8.02-8.06 (m, 2H, H_{py}), 8.58 (s, 1H, O=C-NH), 10.70 (s, 1H, H-OC=N-). ^{13}C NMR □DMSO-d_6, δ (ppm)): 175.02 (-C=O), 155.64 (C=N), 149.02 (C_{Ar}), 148.037 (-C=N_{py}), 137.063(C_{Ar}), 124.24(C_{Ar}), 120.23(C_{Ar}), 27.57(CH_2), 12.25 (-CH_3). ^{13}C NMR{DEPT135} □DMSO-d_6, δ(ppm)): 149.03, 137.06 (C_{Ar}), 124.24 (C_{Ar}), 120.23 (C_{Ar}), 27.71 (CH_2), 12.25 (-CH_3).

2.3 Synthesis of the complexes of H_2L

0.106 g (0.3 mmol) of the ligand were introduced into a flask containing 25 mL of ethanol and 0.0252 g (0.6 mmol) of LiOH·H_2O. An ethanol solution containing 0.6 mmol of transition metal chloride salt (M = Mn, Fe, Co, Ni, Cu, Zn) was added to the mixture. The mixture was refluxed for three hours. After cooling, the solid is recovered by filtration and then washed with cold ethanol (Table 1).

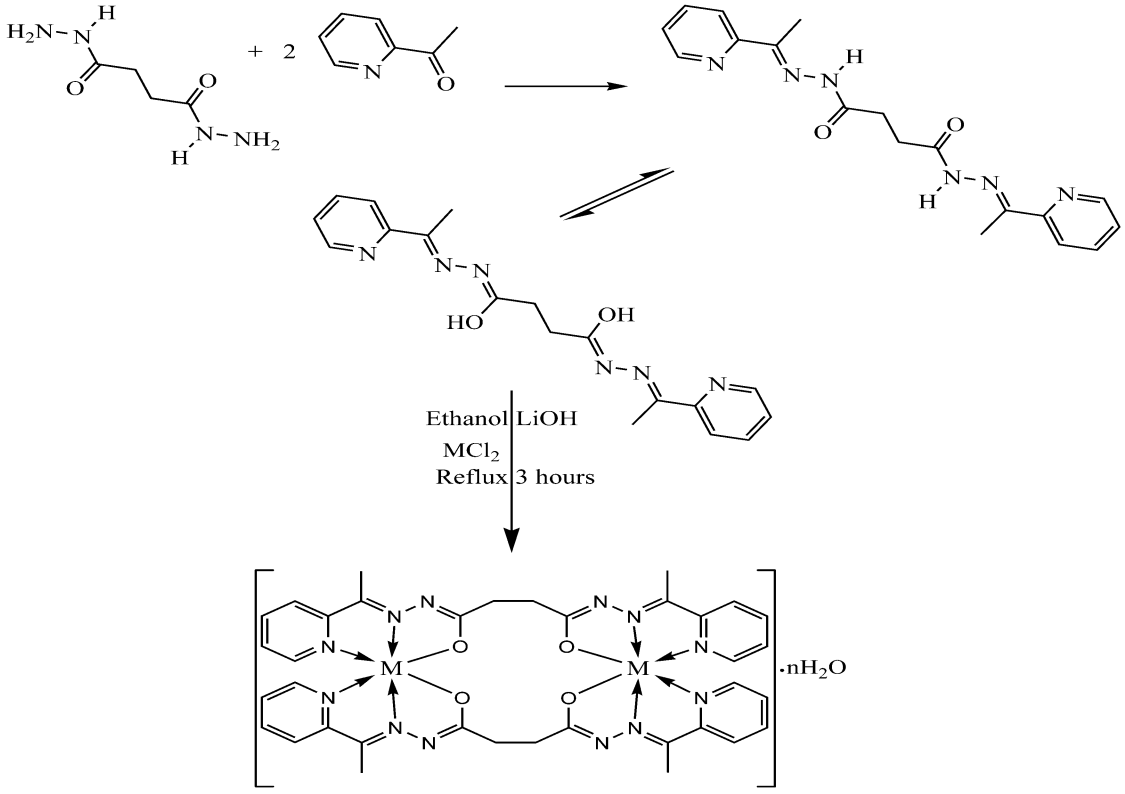

M = Mn, n = 2; M = Fe, n = 4; M = Co, n = 3; M = Ni, n = 3; M = Cu, n =5; M =Zn, n= 2

Scheme 1. Synthetic procedure of the ligand H_2L and its metal transition complexes.

PREVIEW

Table 1. Analytical data, room temperature magnetic moments and conductance of complexes 1-6.

Complexes	Yield (%)	Color	% C Calc. (Found)	% H Calc. (Found)	% N Calc. (Found)	Λ ($\Omega^{-1}\cdot cm^2\cdot mol^{-1}$)	μ_{eff} (μ_B)
H_2L	89	White	61.35 (61.30)	5.72 (5.70)	23.85 (23.82)	-	-
$[(MnL)_2]\cdot 2H_2O$ (**1**) $C_{36}H_{40}Mn_2N_{12}O_6$	50	Green	51.07 (51.01)	4.76 (4.71)	19.85 (19.79)	55	11.84
$[(FeL)_2]\cdot 4H_2O$ (**2**) $C_{36}H_{44}Fe_2N_{12}O_8$	41	Red	48.88 (48.83)	5.01 (4.98)	19.00 (18.93)	27	7.16
$[(CoL)_2]\cdot 3H_2O$ (**3**) $C_{36}H_{42}Co_2N_{12}O_7$	52	Green	49.55 (49.51)	4.85 (4.83)	19.26 (19.21)	8	7.32
$[(NiL)_2]\cdot 3H_2O$ (**4**) $C_{36}H_{42}Ni_2N_{12}O_7$	49	Yellow	49.58 (49.55)	4.85 (4.81)	19.27 (19.22)	5	5.88
$[(CuL)_2]\cdot 5H_2O$ (**5**) $C_{36}H_{46}Cu_2N_{12}O_9$	36	Green	47.11 (47.07)	5.05 (5.01)	18.31 (18.25)	60	3.92
$[(ZnL)_2]\cdot 2H_2O$ (**6**) $C_{36}H_{40}Zn_2N_{12}O_6$	40	White	49.84 (49.80)	4.65 (4.63)	19.37 (19.33)	5	diam

2.4 X-ray structure determination of complex 4

Methanol solution of **4** was left to slow evaporation and yellow crystals suitable for X-ray analyze were formed after three weeks. The details of the X-ray crystal structure solution and refinement are given in Table 3. Measurements were made on a Bruker SMART CCD Area Detector. All data were corrected for Lorentz and polarization effects. Empirical absorption correction was applied. Complex scattering factors were taken from the program package *SHELXTL* [39]. The structures were solved by direct methods, which revealed the position of all non-hydrogen atoms. All the structures were refined on F^2 by a full-matrix least-squares procedure using anisotropic displacement parameters for all nonhydrogen atoms [40]. All hydrogen atoms were located in their calculated positions and refined using a riding model. The contribution of some disordered solvent to the scattering was removed using the *SQUEEZE* routine [41] in *PLATON*. The solvent contribution was not included in the reported molecular weight and density. Molecular graphics were generated using *ORTEP-3* [42].

3. RESULTS AND DISCUSSION

3.1. General study

The infrared spectrum of the ligand shows in the high frequency region, medium intensity bands between 3183 cm^{-1} and 3079 cm^{-1} which are assigned to the ν_{N-H} stretching vibration of the amide moieties. The band at 3010 cm^{-1} is assigned to the aromatic ν_{C-H} vibration. The medium intensity bands between 1570 and 1410 cm^{-1} are assigned to the $\nu_{C=C}$ vibrations of the aromatic rings. A medium intensities bands observed at 1677 cm^{-1} and 1617 cm^{-1} were attributed, respectively, to the $\nu_{C=O}$ and $\nu_{C=N}$ stretching vibrations. The ^1H NMR) spectrum recorded in dimethyl sulfoxide (DMSO-d_6) reveals a singlet signal at

UNDER PEER REVIEW

10.7 ppm HO-C=N-OH and a signal at 8.58 ppm due to O=C-N-H showing that in solution, a partial iminolization of the ligand occured. The signals pointed between 7.39 ppm and 8.06 ppm are attributed to the protons of the aromatic rings. Two singlets pointed at 2.32 ppm and 3.05 ppm are attributed to the proton of the methyl groups and the methylene groups, respectively. The ^{13}C NMR spectrum of the ligand, presents nine signals. Comparing the ^{13}C NMR spectrum with that of $^{13}C\{DEPT\ 135\}$ spectrum, the absence of three signals on the $^{13}C\{DEPT\ 135\}$ spectrum which were present on the ^{13}C spectrum is observed. These signals pointed at 175.017 (C=O), 155.637 (C=N) and 148.037 ppm (C_{Py}-ipso) are due to the tetrasubstituted carbon atoms. The signals of the methyl and methylene carbon atoms are pointed at 12.254 ppm and 27.570 ppm, respectively. Four signals, corresponding to the tertiary carbon atoms of pyridine rings, are pointed at 149.024, 137.063, 124.241 and 120.232 ppm, respectively. Comparison of the FTIR spectrum of the H_2L ligand and those of its complexes reveals a disappearance of the $\nu_{C=O}$ band and a shift towards low frequencies of the $\nu_{C=N}$ bands inn the spectra of comples **1**-**6**. A second $\nu_{C=N}$ band appears after the iminolization of the ligand in solution. This iminolization is facilitated by the adding LiOH during the reaction to facilitate the deprotonation of the -NH groups (Schema 1). Indeed, we point the $\nu_{C=N}$ vibrations in the region [1655 cm^{-1}–1636 cm^{-1}] and [1631 cm^{-1}–1593 cm^{-1}] for complexes **1**-**6**. These data confirm the participation of the nitrogen of the imine functions in the coordination to the metal ion. The vibration attributed to $\nu_{C=N}$ pyridine of the pyridine rings is pointed between 1565 cm^{-1} and 1597 cm^{-1} on all the spectra of the complexes. For all complexes, the two identical arms of the ligand, acts similarly, and coordinates to two metal ions through the alcoholate oxygen atoms, the azomethine nitrogen atoms and the pyridine nitrogen atoms. The presence of uncoordinated water molecules is indicated by the ν_{O-H} bands located between 3435 cm^{-1} and 3555 cm^{-1} [43].

Table 2. Main FTIR and UV-visible bands for H_2L and complexes 1-6.

Compound	ν(O-H)	ν(N-H)	ν(N-H)	ν(C=O)	ν(C=N)		ν(C=Npy)	ν(N-N)	λ(nm)
H_2L		3183	3079	1677	-	1617	1579	1045	210, 265, 296
(**1**)	3439	-	-	-	1655	1631	1595	1032	213, 263, 296, 345, 446, 537
(**2**)	3446	-	-	-	1624	1611	1597	1029	208, 261, 295, 342, 395-610
(**3**)	3531	-	-	-	1652	1620	1595	1044	207, 267, 299, 350, 477, 915
(**4**)	3459	-	-	-	1650	1600	1595	1041	213, 266, 295, 348, 425, 814
(**5**)	3455	-	-	-	1658	1613	1596	1033	212, 269, 300, 340, 550-660
(**6**)	3439	-	-	-	1636	1593	1565	1039	208, 265, 298

3.2. Magnetism

Magnetic study at room temperature has shown that these complexes are binuclear. For the Mn(II) complex (**1**), the magnetic moment value of 11.84 μ_B is consistent with a octahedral dinuclear complex without exchange between the two high-spin centers of d^5 configuration [44]. The Fe(II) complex (**2**) has a μ_{eff} of 7.16 μ_B. This value is close to the spin-only value for two non-coupled high-spin iron(II) [45]. These two ions are located in an octahedral environment. The cobalt complex (**3**) has two high-spin Co(II) ions in octahedral environmment which are magnetically isolated as indicated by the μ_{eff} value of 7.32 μ_B [46]. The magnetic moment value (μ_{eff} = 5.88 μ_B) of complex (**4**) indicates the presence of two Ni(II) ions in an octahedral environment that are magnetically isolated from each other [47]. Complex (**5**) is a Cu(II) dinuclear complex without magnetic exchange (μ_{eff} = 3.92 μ_B) in which the two matal ion are located in octahedral geometry [48]. Complex (**6**) of zinc is diamagnetic as expected for a d^{10} configuration.

3.3. Molar conductance

All complexes exhibit molar conductivities between 5 and 60 $\Omega^{-1}\cdot cm^2\cdot mol^{-1}$ which indicate that complexes **1**-**6** have neutral in nature. These values remain almost constant over time, indicating the good stability of the complexes in DMF solutions [49].

UNDER PEER REVIEW

3.4. Electronic spectra

The electronic spectra data of H_2L and the complexes **1**-**6** are shown in table 2. The spectrum of the ligand H_2L exhibits three bands at 210 nm, 265 nm, and 296 nm which were assigned to $\pi\rightarrow\pi^*$ transitions. These bands are present in the electronic spectra of the complexes **1**-**6**. The complexes **1**-**5** have an intense absorption band [340 nm – 350 nm] attributable to the metal-to-ligand charge-transfer (MLCT) transition. The Mn(II) complex (**1**) exhibits two additional bands at 446 nm and 537 nm which are assigned to the $^6A_{1g}\rightarrow{}^4T_{1g}$ and $^6A_{1g}\rightarrow{}^4T_{2g}$ transitions, respectively, corresponding to octahedral geometry for the Mn(II) ion [50]. The Iron complex (**2**) showed a d-d transtion at 395-610 nm attributed to the $^2E_g\rightarrow{}^2T_{2g}$ for d^6 configuration of Fe(II) in an octahodral environment [51]. The electronic spectrum of the cobalt complex (**3**), displays two bands at 477 nm and 915 nm, which may reasonably be assigned to the $^4T_{1g}$ (F)$\rightarrow{}^4T_{2g}$ (P) and $^4T_{1g}$ (F)$\rightarrow{}^4T_{2g}$ (F) transitions, respectively, suggesting an octahedral geometry around the Co(II) ion [52]. The electronic spectrum of the nickel complex (**4**), shows two bands located at 425 nm and 814 nm which may be ascribed to the $^3A_{2g}$(F)$\rightarrow{}^3T_{1g}$(P) and $^3A_{2g}$(F)$\rightarrow{}^3T_{1g}$(F) transitions, respectively indicating an octahedral environment [53, 54]] around the Ni(II) ion. The UV-visible spectrum of Cu complex (**5**) showed a broad band in the region 550-660 nm which envelops the three transitions $^2B_{1g}\rightarrow{}^2A_{1g}$, $^2B_{1g}\rightarrow{}^2B_{2g}$ and $^2B_{1g}\rightarrow{}^2E_g$. The broadness of the band is propably due due to the Jahn-Teller effect [55]. These observations suggest that the copper(II) is situated in a distorted octahedral environment [56]. On the basis of elemental analysis, magnetic moment and conductance measurements, UV-Visible spectra and FTIR spectra, each molecule of complexes **1**-**6** contains two organic ligands acting in hexadentate fashion with two metal ions. Each metal ion is coordinated by two alcoolate oxygen atoms, two nitrogen azomethine atoms and two nitrogen atoms from pyridine ring. Uncoordinated water molecules are present in the structures of the complexes. The suggested structure of the complexes are octahedral in nature as shown in Scheme 1.

3.5. Description of the crystal structure of the complex 4

The molecular structure of the nickel(II) complex (**4**) is given in Figure 1. Selected bond lengths and angles are listed in Table 4. The nickel(II) complex crystallizes in the $P\bar{1}$ space group of the triclinic system. The asymmetric unit of the structure contains two Ni(II) ions and two ligand molecules in its L^{2-} form. Each Ni(II) ion of the complex (**4**) is situated in a distorted octahedral geometry, having the N_4O_2 coordination environment. The coordination of the Ni(II) ion is filled by two O atom of an iminol group, two azomethine nitrogen atoms and two nitrogen atoms from pyridine rings. In each ligand molecule, the flexible alkyl linker chain shows *syn* conformation and the two mono deprotonated tridentate arms of the ligand adopt a *cis* configuration. This behavior of the ligand is observed in similar Schiff base [57]. The structural parameters of the two arms are slightly different. The basal planes of the polyhedron around the Ni1 and Ni2 ions are occupied by O2, N5, N6 and N8 for Ni1 and O4, N2, N10, N11, for Ni2 while the apical positions are occupied by O3 and N7 for Ni1 and O1 and N1 for Ni2. The *cissoid* angles which are in the range [77.64(9)° – 107.71(10)°] and the *transoid* angle 173.28(10)° and 156.59(9)° for Ni1 and 174.37(10)° and 155.72(8)° for Ni2, deviate severely from the ideal values of 90° and 180°, respectively, as expected for a perfect octahedral geometry. The angles subtended by atoms in apical positions [O3—Ni1—N7 = 154.74(9)° and O1—Ni1—N1 = 155.56(8)°] are far from the ideal value of 180°. The octahedral environments around the Ni1 and Ni2 are severely distorted. The sum of the angle subtended by the atoms in the basal planes are 360.08° for Ni1 and 360.16° for Ni2. Each tridentate arm of the ligand forms two five membered rings of type NiNCCN and NiNNCO with the Ni. The chelate ring are quite planar as shown by the small torsion angles (Table 5). The bite angle values resulted are in the range [76.68(9)° – 78.61(10)°]. The mean planes defined by the atoms which form the two six membered ring for each arms of the two ligands are quite perpendicular as shown by the dihedral angle values of 88.58° for Ni1 [Ni1/O3/C26/N9/N8/C24/C23/N7 *vs* Ni1/O2/C11/N4/N5/C12/C14/N6] and 87.24° for Ni2 [Ni2/O1/C8/N3/N2/C6/C5/N1 *vs* Ni2/O4/C29/N12/N13/C30/C32/N10]. The apical bond lengths Ni—O [O3—Ni1 = 2.153(2) Å and O1—Ni2 = 2.122(2) Å] are the longest distances around these two nickel atoms. The equatorial bond lengths Ni—N_{py} [Ni1—N6 = 2.089(3) Å and Ni2—N10= 2.082(2) Å] are longer than the equatorial Ni—N_{imino} distances which are 1.972(2) Å [Ni1—N5], 2.004(2) Å [Ni1—N8], 1.982(3) Å [Ni2—N2] and 1.978(3) Å [Ni2—N11]. These values are close proximity to the values reported for the complex bis{*N*-[1-(pyridin-2-yl-N)ethylidene]pyridine-4-carbohydrazonato-k^2N',*O*}nickel(II)–2,5-dichloroterephthalic acid [58]. The distance Ni—Ni value is 5.991(2) Å. The

UNDER PEER REVIEW

distances C—O [O1—C8 = 1.252(4) Å, O4—C29 = 1.257(4) Å, O3—C26 = 1.241(3) Å, O2—C11 = 1.266(3) Å] and C—N [C8—N3 = 1.357(4) Å, C29—N12 = 1.342(3) Å, C26—N9 = 1.364(3) Å, C11—N4 = 1.339(4) Å] are compatible to the values reported with similar ligand [59].

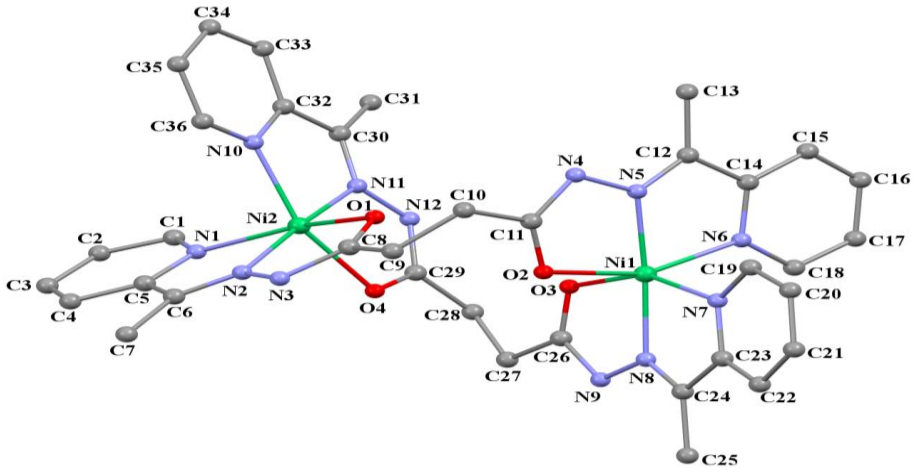

Figure 1. Crystal structure of the complex (4). Displacement ellipsoids are drawn at the 30% probability level and H atoms are omitted for clarity.

Table 3. Crystallographic data and refinement parameters for complex 4.

Chemical formula	$C_{36}H_{36}N_{12}Ni_2O_4$
M_r	818.15
Crystal system, space group	Triclinic, $P\bar{1}$
Temperature (K)	173
a, *b*, *c* (Å)	10.647 (2), 14.030 (3), 18.077 (4)
α, β, γ (°)	69.33 (3), 86.34 (3), 70.01 (3)
V (Å^3)	2369.3 (11)
Z	2
Radiation type	Mo $K\alpha$
μ (mm^{-1})	0.84
Crystal size (mm)	0.40 × 0.30 × 0.20
No. of measured, independent and observed [$I > 2\sigma(I)$] reflections	74467, 9777, 8735
R_{int}	0.035
$R[F^2 > 2\sigma(F^2)]$, $wR(F^2)$, S	0.055, 0.174, 1.04
No. of reflections	9777
No. of parameters	491
H-atom treatment	H-atom parameters constrained
$\Delta\rho_{max}$, $\Delta\rho_{min}$ (e Å^{-3})	0.62, −0.89

Table 4. Selected bond lengths (Å) and bond angles (°) of complex 4.

Ni1—N5	1.971 (2)	N5—Ni1—N8	173.28 (10)
Ni1—N8	2.004 (3)	O2—Ni1—N6	156.59 (9)
Ni1—N7	2.069 (3)	N7—Ni1—O3	154.74 (9)
Ni1—O2	2.070 (2)	N5—Ni1—N7	99.35 (10)
Ni1—N6	2.089 (3)	N8—Ni1—N7	78.08 (10)
Ni1—O3	2.153 (2)	N5—Ni1—O2	78.12 (9)
Ni2—N11	1.977 (2)	N11—Ni2—N2	174.37 (10)
Ni2—N2	1.982 (2)	N10—Ni2—O4	155.72 (8)
Ni2—N10	2.082 (3)	N1—Ni2—O1	155.56 (8)
Ni2—N1	2.082 (2)	N11—Ni2—N10	78.20 (9)
Ni2—O4	2.105 (2)	N2—Ni2—N10	106.72 (10)
Ni2—O1	2.122 (2)	N11—Ni2—N1	98.78 (9)

Table 5. Selected torsion angles (°) in complex 4.

Ni1–O2–C11–N4	1.7(4)
Ni1–N5–C12–C14	0.6(3)
Ni1–N7–C23–C24	6.0(3)
Ni1–O3–C26–N9	-2.8(3)
Ni1–N5–N4–C11	-2.3(3)
Ni1–N6–C14–C12	0.4(3)
Ni1–N8–C24–C23	-0.5(3)
Ni1–N8–N9–C26	-0.3(3)
Ni2–N10–C32–C30	1.4(3)
Ni2–N11–C30–C32	7.9(3)
Ni2–N11–N12–C29	-3.8(3)
Ni2–O4–C29–N12	-0.8(4)
Ni2–N1–C5–C6	-4.5(3)
Ni2–N2–C6–C5	-2.2(4)
Ni2–N2–N3–C8	4.1(3)
Ni2–O1–C8–N3	-2.7(4)

4. CONCLUSION

The new ligand *N*'^{1},*N*'^{4}-bis(1-(pyridin-2-yl)ethylidene)succinohydrazide was synthetized and structurally characterized. The ligand was used for chelation with metal ions with Mn(II), Fe(II), Co(II), Ni(II), Cu(II) and Zn(II) ions. The complexes are characterized by FTIR and UV-visible spectroscopies, room temperature magnetic moments measurements, conductivity measurement and X-ray diffraction for the Ni(II) complexes. The ligand acts as dinegative hexadentate in the all the complexes. In each complex two ligand molecules coordinate two metal ions. Each ligand possesses two arms which coordinates one metal ion in tridentate fashion trough one azomethine nitrogen atom, one pyridine nitrogen atom and one iminolate oxygen atom. Octahedral geometries are proposed for the complexes **1**-**6**.

Supplementary data

CCDC–2381435 contains the supplementary crystallographic data for the complex **4**. These data can be obtained free of charge via www.ccdc.cam.ac.uk/conts/retrieving.html, or from the Cambridge Crystallographic Data Centre,

UNDER PEER REVIEW

12 Union Road, Cambridge CB2 1EZ, UK (Telephone: +44–01223–762910; Fax: +44–1223–336033; or E-mail: deposit @ccdc.cam.ac.uk).

In Memoriam

Cheikh Halidou KANE 1963–2021. The death of Dr. KANE has deeply shocked us. Dr. KANE was a very talented chemist who was deeply involved in research and supervision of doctoral students. His contribution is greatly missed by our team. This article is dedicated to his memory.

Disclaimer (Artificial intelligence)

1. Author(s) hereby declares that NO generative AI technologies such as Large Language Models (ChatGPT, COPILOT, etc.) and text-to-image generators have been used during writing or editing of manuscripts.
2. Author(s) hereby declares that generative AI technologies such as Large Language Models, etc. have been used during writing or editing of manuscripts. This explanation will include the name, version, model, and source of the generative AI technology and as well as all input prompts provided to the generative AI technology

Details of the AI usage are given below:

UNDER PEER REVIEW

References

1. Yang Y, Wang Y, Gou Q, Zhang Y, Wu Y, Luo Y. Synthesis of thiophene Schiff base functionalized UiO-66 for enhanced Cu(II) ion adsorption capacity and selectivity. J. Solid State Chem. 2024; 332:124599.
2. Singh G, Devi S, Singh A, Mohit, Devi A, Diksha, Sharma S, Esteban MA, Espinosa-Ruíz, C. 1,2,3-Triazole appended Schiff base functionalized silanes: A colorimetric sensor of Al (III) and a potent inhibitor of butyrylcholinesterase in Alzheimer's diseases via molecular docking. Inorg. Chim. Acta 2024;572:122269.
3. Zhang H, Wang P, Shan W, Xiong Y, Xing Z, Yu H. (2024). Synthesis of Schiff base-functionalized ordered mesoporous silica for effective adsorption of Re(VII). Colloids Surf., A 2024;690:133792.
4. Xu H, Xu Y, Zheng X, Zhang S, Guo Y. Removal of Hg(II) with MgAl-layered double hydroxide functionalized by schiff base ligands: Application and condition optimization. Chemosphere 2024;364:142972.
5. Shatir TM, Aly KA, Ebrahium MM, Saddeek YB, Kumar ER. Linear and non-linear optical and dielectric properties of transition metals complexes films derived from Azo-Schiff base for photovoltaic applications. J. Mol. Liq. 2024;401:124636.
6. Pramanik S, Chattopadhyay S. An overview of copper complexes with diamine-based N_4 donor bis-pyridine Schiff base ligands: Synthesis, structures, magnetic properties and applications. Inorg. Chim. Acta 2023;552:121486.
7. Tao R, Wang Y, Zhang N, Zhang L, Khan MS, Xu H, Zhao J, Qi Z, Chen Y, Lu Y, Wan, K, Wand Y, Jiang J. Bioactive chitosan-citral Schiff base zinc complex: A pH-responsive platform for potential therapeutic applications. Int. J. Biol. Macromol. 2024;261:129857.
8. Adam MSS, Abdel-Rahman OS, Makhlouf MM. Metal ion induced changes in the structure of Schiff base hydrazone chelates and their reactivity effect on catalytic benzyl alcohol oxidation and biological assays.J. Mol. Struct. 2023;1272:134164.
9. Zhang X, Ma J, Zou B, Ran L, Zhu L, Zhang H, Ye Z, Zhou L. Synthesis of a novel bis Schiff base chelating resin for adsorption of heavy metal ions and catalytic reduction of 4-NP. React. Funct. Polym. 2022;180:105409.
10. Nagaraj R, Murugesan S, Jeyaraj D. R, Arumugam S, Shunmugasundaram G, Radhakrishnan NA. Spectroscopic studies on DNA interaction and anticancer activities of pharmacologically active pyrimidine derivative mixed ligand Co(II) and Ni(II) complexes. J. Mol. Struct. 2022;1252:132079.
11. Das S, Das M, Bag A, Laha S, Samanta BC, Choudhury I, Bhattacharya N, Maity T. Selective recognition of Zn(II) by a novel Schiff base chemosensor with the formation of an AIE active Zn(II) complex having picric acid detection ability: Application in live cell imaging study. J. Photochem. Photobiol., A 2024;447:115214.
12. Sayed FN, Ashmawy AM, Saad SM, Omar MM, Mohamed GG. Design, spectroscopic characterization, DFT, molecular docking, and different applications: Anti-corrosion and antioxidant of novel metal complexes derived from ofloxacin-based Schiff base. J. Organomet. Chem. 2023;993:122698.

13. Janjua UU, Pervaiz M, Ali F, Saleem A, Ashraf A, Younas U, Iqbal M. Schiff base derived Mn(II) and Cd(II) novel complexes for catalytic and antioxidant applications. Inorg. Chem. Commun. 2023;157:111233.
14. Norouzi M, Noormoradi N, Mohammadi M. Nanomagnetic tetraaza (N_4 donor) macrocyclic Schiff base complex of copper(II): synthesis, characterizations, and its catalytic application in Click reactions. Nanoscale Adv. 2023;5(23):6594–6605.
15. Zhang HZ, Zhou HW, Zhao SZ, Chen LW, Qin CY, Li YH, Wang, S. Cooperative effects of ligands and Counteranions in mononuclear Manganese(III) Schiff-base spin crossover complexes. J. Mol. Struct. 2024;1307:138031.
16. Hafidi R, Messai A, Chebbah M, Kadri R, Labidi NS, Kadri M. A new mononuclear copper (II) complex with an *O*,*N*,*O*'-tridentate Schiff base ligand: Synthesis, structural, Hirshfeld surface, electrochemical and theoretical studies. Inorg. Chem. Commun. 2024;159:111689.
17. Middya P, Medda D, Chattopadhyay S. An overview of the synthesis, structures and applications of di and polynuclear zinc-salen complexes with Zn_2O_2 cores. Inorg. Chim. Acta 2023;554:121540.
18. Luo Y, Wang J, Ding X, Ni R, Li M, Yang T, Wang T, Wang J, Jing C, You Z. Syntheses, crystal structures and antimicrobial activities of polynuclear Co^{II}, Ni^{II} and Zn^{II} complexes derived from the *N*,*N*'-bis(4-fluorosalicylidene)-1,3-propanediamine Schiff base. Inorg. Chim. Acta 2021;516:120146.
19. Dong J, Wan T, Li K, Kong X, Shen Q, Wu H. Mononuclear Dy(III)/heteropolynuclear Zn(II)–Dy(III) Schiff base complexes: Synthesis, structures, fluorescence and antioxidant properties. J. Mol. Struct. 2022;1264:133340.
20. Bandyopadhyay D, Karmakar D, Pilet G, Fleck M. Synthesis and crystal structure of two new heteropolynuclear $[Ni^{II}Cd^{II}Cd^{II}Ni^{II}]$ and $[Ni^{II}Cd^{II}Ni^{II}]$ Schiff base complexes involving bridging chlorine and oxygen functions. Polyhedron 2011;30(16):2678–2683.
21. Ding DD, Gao T, Sun O, Li GM, Wu YH, Xu MM, Zou XY, Yan PF. Heteropolynuclear Schiff-base complexes Cu–Ln–Fe (Ln=Sm Pr) with magnetic property. Inorg. Chem. Commun. 2015;51:21–25.
22. Danilescu O, Bourosh P, Kulikova OV, Chumakov YM, Bulhac I, Croitor L. Dihydrazone Schiff base ligands – appropriate chemosensors for Cd(II) detection. Inorg. Chem. Commun. 2022;146:110199.
23. Sahu M, Manna AK, Patra GK. A dihydrazone based conjugated bis Schiff base chromogenic chemosensor for selectively detecting copper ion. Inorg. Chim. Acta 2021;517:120199.
24. Pervaiz M, Sadiq A, Sadiq S, Saeed Z, Imran M, Younas U, Bukhari SM, Khan, RRM, Rashid A, Adnan A. Design and synthesis of Schiff base Homobimetallic-Complexes as promising antimicrobial agents. Inorg. Chem. Commun. 2022;137:109206.
25. El-Asmy AA, El-Gammal OA, Radwan HA. Synthesis, characterization and biological study on Cr^{3+}, ZrO^{2+}, HfO^{2+} and UO_2^{2+} complexes of oxalohydrazide and bis(3-hydroxyimino)butan-2-ylidene)-oxalohydrazide. Spectrochim. Acta, Part A 2010;76(5):496–501.
26. Adam MSS, Alghanim AlSI, Abdel-Rahman OS, Makhlouf MM. Diisatin malonyldihydrazone complexes of high valent oxovanadium and oxozirconium ions for bio-chemical effectiveness and catalytic thiophene oxidation. J. Mol. Liq. 2024;397:124183.
27. El-Boraey HA, El-Domiaty AM. Influences of γ-ray irradiation on physico-chemical, structural, X-ray diffraction, thermal and antimicrobial activity of some γ-irradiated *N*′,*N*‴-((Z)-ethane-1,2-diylidine)bis(2-aminobenzohydrazide) metal complexes. Appl. Radiat. Isot. 2021;174:109774.
28. Sinha A, Chaudhary R, Reddy DS, Kongot M, Kurjogi MM, Kumar A. ON donor tethered copper (II) and vanadium (V) complexes as efficacious anti-TB and anti-fungal agents with spectroscopic approached HSA interactions. Heliyon 2022;8(8):e10125.
29. Kamat V, Kokare D, Naik K, Kotian A, Naveen S, Dixit SR, Lokanath NK, Joshi SD, Revankar VK. Transition metal complexes of 2-(2-(1*H*-benzo[d]imidazol-2-yl)hydrazono)propan-1-ol: Synthesis, characterization, crystal structures and anti-tuberculosis assay with docking studies. Polyhedron 2017;127:225–237.
30. Ebrahimipour SY, Sheikhshoaie I, Castro J, Haase W, Mohamadi M, Foro S, Sheikhshoaie M, Esmaeili-Mahani S. A novel cationic copper(II) Schiff base complex: Synthesis, characterization, crystal structure, electrochemical evaluation, anti-cancer activity, and preparation of its metal oxide nanoparticles. Inorg. Chim. Acta 2015;430:245–252.
31. Patel SK, Patel RN, Patel AK, Patel N, Choquesillo-Lazarte D. Copper hydrazone complexes with different nuclearties and geometries: Synthesis, characterization, single crystal structures, Hirshfeld analysis and superoxide dismutase mimetic activities. J. Mol. Struct. 2022;1257:132545.
32. Patel AK, Jadeja RN, Butcher RJ, Kesharwani MK, Kästner J, Muddassir M. New copper(II) complexes with (*Z*)-*N*′-(2-hydroxynaphthalen-1-ylmethylene)acetohydrazide]: X-ray structure, Hirshfeld analysis, X-band

UNDER PEER REVIEW

electron paramagnetic resonance spectra, TD-DFT calculations and superoxide dismutase mimetic activity. Polyhedron 2021;195:114969.
33. Zengin A, Serbest K, Emirik M, Özil M, Menteşe E, Faiz Ö. Binuclear Cu(II), Ni(II) and Zn(II) complexes of hydrazone Schiff bases: Synthesis, spectroscopy, DFT calculations, and SOD mimetic activity. J. Mol. Struct. 2023;1278:134926.
34. Diop A, Sarr M, Diop M, Thiam IE, Barry AH, Coles S, Orton J, Gaye M. Metal transition complexes of tridentate Schiff base ligands derived from 2-hydrazinopyridine: synthesis, spectroscopic characterization and X-ray structures. Transition Met. Chem. 2019;44(5):415–423.
35. Gueye MN, Dieng M, Lo D, Thiam IE, Barry AH, Gaye M, Sall AS, Retailleau P. Synthesis, physical studies and crystal structure determination of Y(III) and Er(III) complexes of 1-(pyridin-2-yl)-2-(pyridine-2-ylmethylene)hydrazine. Eur. J. Chem. 2017;8(2):137–143.
36. Tamboura FB, Diouf O, Barry AH, Gaye M, Sall AS. Dinuclear lanthanide(III) complexes with large-bite Schiff bases derived from 2,6-diformyl-4-chlorophenol and hydrazides: Synthesis, structural characterization and spectroscopic studies. Polyhedron 2012;43(1):97–103.
37. Gueye A, Tamboura FB, Sy A, Gaye M, Gruber N, Jouaiti A. Six New Transition Metal Mononuclear Complexes Of *N*'-(5- bromo-2-hydroxybenzylidene)nicotinohydrazide Schiff Base. Synthesis, Spectroscopic Characterization And X-ray structure Determination of the Zinc(II) Complex. IOSR J. Appl. Chem. 2019;12:24–30.
38. Kane CH, Tinguiano D, Tamboura FB, Thiam IE, Barry AH, Gaye M, Retailleau P. Synthesis and characterization of novel M(II) (M = Mn(II), Ni(II), Cu(II) or Zn(II)) complexes with tridentate N_2,O-donor ligand (*E*)-2-amino-*N*'-[1-(pyridin-2-yl)- ethylidene]benzohydrazide. Bull. Chem. Soc. Ethiop. 2016;30(1):101–110.
39. Sheldrick GM. SHELXT – Integrated space-group and crystal-structure determination. Acta Crystallogr., Sect. A: Found. Adv. 2015;71(1):3–8.
40. Sheldrick GM. Crystal structure refinement with SHELXL. Acta Crystallogr., Sect. C: Struct. Chem. 2015;71(1):3–8.
41. Spek AL. PLATON SQUEEZE: a tool for the calculation of the disordered solvent contribution to the calculated structure factors. Acta Crystallogr., Sect. C: Struct. Chem. 2015;71(1):9–18.
42. Farrugia LJ. WinGX and ORTEP for Windows: an update. J. Appl. Crystallogr. 2012;45(4):849–854.
43. Kumar DS, Alexander V. Synthesis of lanthanide(III) complexes of chloro- and bromo substituted 18-membered tetraaza macrocycles. Polyhedron 1999;18(11):1561–1568.
44. Brudenell SJ, Spiccia L, Bond AM, Fallon GD, Hockless DCR, Lazarev G, Mahon PJ, Tiekink ERT. Structural, Spectroscopic, and Electrochemical Studies of Binuclear Manganese(II) Complexes of Bis(pentadentate) Ligands Derived from Bis(1,4,7-triazacyclononane) Macrocycles. Inorg. Chem. 2000;39(5):881–892.
45. Hofmann A. J, Jandl C, Hess CR. Structural Differences and Redox Properties of Unsymmetric Diiron PDIxCy Complexes. Eur. J. Inorg. Chem. 2020;2020(5):499–505.
46. Al-Shaalan NH. Synthesis, Characterization and Biological Activities of Cu(II), Co(II), Mn(II), Fe(II), and UO2(VI) Complexes with a New Schiff Base Hydrazone: O-Hydroxyacetophenone-7-chloro-4-quinoline Hydrazone. Molecules 2011;16(10):8629–8645.
47. Xu Z, Thompson LK, Miller DO, Clase HJ, Howard JAK, Goeta AE. Spiral Dinuclear Complexes of Tetradentate N_4 Diazine Ligands with Mn(II), Fe(II), Fe(III), Co(III), and Ni(II) Salts. Inorg. Chem. 1998;37(14):3620–3627.
48. Xu Z, Thompson LK, Matthews CJ, Miller DO, Goeta AE, Wilson C, Howard JAK, Ohba M, Ōkawa H. Dinuclear and tetranuclear copper(II) complexes with bridging (N–N) diazine ligands: variable magnetic exchange topologies. J. Chem. Soc., Dalton Trans. 2000:69–77.
49. Geary WJ. The use of conductivity measurements in organic solvents for the characterisation of coordination compounds. Coord. Chem. Rev. 1971;7(1):81–122.
50. Khan TA, Naseem S, Azim Y, Parveen S, Shakir M. Metal-ion directed synthesis of binuclear octaazamacrocyclic complexes of manganese(II), cobalt(II), nickel(II), copper(II) and zinc(II) and their physico-chemical studies. Transition Met. Chem. 2007;32(6):706–710.
51. Ullah MR, Hossain MJ, Hossain A. The Influence of a New-Synthesized Complex Compounds of Ni (II), Cu (II) And Fe (II) Containing A Ligand Having Tetraoxotetrahydrazin Moity on Some Pathogenic Bacteria. IOSR J. Appl. Chem. (IOSR-JAC) 2013;4(4):51–59.
52. Singh K, Thakur R, Kumar V. Co(II), Ni(II), Cu(II), and Zn(II) complexes derived from 4-[3-(4-bromophenyl)-1-phenyl-1*H*-pyrazol-4-ylmethylene-amino]-3-mercapto-6-methyl-5-oxo-1,2,4-triazine. Beni-Suef Univ. J. Basic Appl. Sci. 2016;5(1):21–30.

UNDER PEER REVIEW

53. Belle C, Bougault C, Averbuch MT, Durif A, Pierre JL, Latour JM, Le Pape L. Paramagnetic NMR Investigations of High-Spin Nickel(II) Complexes. Controlled Synthesis, Structural, Electronic, and Magnetic Properties of Dinuclear vs Mononuclear Species. J. Am. Chem. Soc. 2001;123(33):8053–8066.
54. Odunola, OA, Adeoye, IO, Woods, JAO, Gelebe, AC. Synthesis and Characterization of Nickel(II) Complexes of Benzoic Acid and Methyl Substituted Benzoic Acid Hydrazides and X-Ray Structure of $Ni[C_6H_5CONHNH_2]_3Cl_2{\cdot}3CH_3OH$. Synth. React. Inorg. Met.-Org. Chem. 2003;33(2):205–221.
55. Conradie J. Jahn-Teller effect in high spin d^4 and d^9 octahedral metal-complexes. Inorg. Chim. Acta 2019;486:193–199.
56. Liu H, Wang H, Feng G, Niu D, Lu Z. Self-assembly of copper(II) complexes with substituted aroylhydrazones and monodentate N-heterocycles: synthesis, structure and properties. J. Coord. Chem. 2007;60(24):2671–2678.
57. El-Asmy AAE, Jeragh B, Ali MS. Synthesis and characterization of tri- and tetra-metallic complexes of *N*'^{1},*N*'^{4}-bis((*E*)-3,4-dihydroxybenzylidene)-succinohydrazide. Eur. J. Chem. 2016;7(1):81–90.
58. Nakanishi T, Sato O. Crystal structures of two nickel compounds comprising neutral Ni^{II} hydrazone complexes and dicarboxyic acids. Acta Crystallogr., Sect. E: Crystallogr. Commun. 2017;73(2):103–106.
59. Sedaghat T, Aminian M, Rudbari H. A, Bruno, G. Dinuclear organotin(IV) complexes with bis-acyl-hydrazones containing flexible linker: Synthesis, spectroscopic investigation and crystal structure of dimethyl- and diphenyltin(IV) complexes with succinic dihydrazones. J. Organomet. Chem. 2014;754:26–31.

UNDER PEER REVIEW